Using invariant altitude (h_{inv}) for mapping of the radiation belt fluxes in the low-altitude environment

Juan Cabrera[1] and Joseph Lemaire[1,2]

Received 24 June 2006; revised 7 December 2006; accepted 9 December 2006; published 26 April 2007.

[1] Mapping of the radiation belt environment in the classical (B, L) invariant coordinates is rather poorly resolved at low altitudes where the SAMPEX and DEMETER missions are collecting scientific data. This lack of adequate spatial resolution at low altitudes has been pointed out since 1986. A simple solution to this standing problem is proposed in this article. We recall alternative coordinates that were proposed in the 90s to improve the spatial resolution of binning meshes and radiation belt maps in the low-altitude region, i.e., near the atmospheric cutoff. Next, we define a new coordinate: the "invariant altitude," h_{inv}, that we recommend instead of B or other invariant drift shell coordinates like B/B_0 or α_0, the equatorial pitch angle. In McIlwain's reference dipole, the new coordinate, h_{inv}, corresponds to the altitude (in units of km) of mirror points of particles which have given values of B and I or L, calculated by using a geomagnetic field model like the International Geomagnetic Reference Field. The advantages and limitations of the new h_{inv} coordinate are presented. For illustration, the distributions of the omnidirectional fluxes of electrons and protons predicted by the standard AE8 and AP8 radiation belt models are displayed using this new invariant coordinate, as well as by using alternative invariant coordinates like B/B_0 or α_0. A set of orbits of the SAMPEX, DEMETER, and CRRES spacecraft are displayed in these different coordinate systems to illustrate the advantage of using the invariant altitude h_{inv} to map the radiation belt environment at low altitudes.

Citation: Cabrera, J., and J. Lemaire (2007), Using invariant altitude (h_{inv}) for mapping of the radiation belt fluxes in the low-altitude environment, *Space Weather*, *5*, S04007, doi:10.1029/2006SW000263.

1. Introduction

[2] In recent issues of *Space Weather*, several articles have reported workshops and news dealing with radiation belt (RB) modeling issues, RB damages, and RB risks. Empirical models for the RB environment have been developed over the last decades at NASA Goddard Space Flight Center (GSFC) and Marshall Space Flight Center, at The Boeing Company, at the Air Force Geophysics Laboratory, and at the Belgian Institute for Space Aeronomy (BISA). These statistical models generally provide the omnidirectional energy spectrum of energetic electrons and protons in space and averaged over extended periods of time. Therefore most of these models are static and come in pairs: the first ones for solar maximum or geomagnetically active periods and the others for solar minimum or quiet periods. Probabilistic models have been proposed in the recent years, offering empirical models for a whole range of solar activity levels [*Xapsos et al.*, 2002]. Physics-based transport codes using the data assimilation technique have also been developed recently to model the environment of energetic RB electrons [*Bourdarie et al.*, 2005].

[3] These newer models must of course still be tested and validated, and possibly improved, using observations from forthcoming missions in the magnetosphere during future solar cycles. The efforts at NASA Goddard Space Flight Center to develop a new generation of trapped RB models has been presented by *Fung* [1996]. A framework for the next-generation radiation belt models based on the determination of joint probability distributions has recently been discussed in *Space Weather* by *O'Brien* [2005].

[4] The early NASA radiation belt models AE8-MIN and AE8-MAX and AP8-MIN and AP8-MAX were developed until 1972 [*Vette*, 1991]. The acronym A in AE8 and AP8 stands for Aerospace Corporation, 8 corresponds to the eighth and last version of these models, and MIN and MAX stand for minimum and maximum solar activity conditions, respectively; E stands for electrons, and P stands for protons.

[5] In the AE8 and AP8 radiation belt models, appropriate energy bins were selected to cover the spectrum ranging from 40 keV to 7 MeV for the energetic electrons and from 100 keV to 400 MeV for the trapped protons. Suitable grids of drift shell coordinates had been adopted

[1]Centre for Space Radiations, Louvain-la-Neuve, Belgium.
[2]Belgian Institute for Space Aeronomy, Brussels, Belgium.

by Jim Vette and coworkers at National Space Science Data Center (NSSDC)/World Data Center A Rockets and Satellites to cover adequately all relevant regions of the magnetosphere radiation belts for electrons and protons. These energetic electron and proton fluxes were collected by a number of different types of detectors on several satellites in the 60s. Similar empirical RB models have also been developed at the Sobeltsyn Institute of Nuclear Physics in Moscow. They have been compared to the NASA models by *Beliaev and Lemaire* [1996].

[6] Despite their limitations, pointed out in several papers, including that of *O'Brien* [2005], these early statistical RB models have been intensively used for over three decades. They will still be employed for some time, as references for future spacecraft design and proposal evaluations, because of their comprehensive spatial coverage of the whole magnetosphere. This is likely to remain so until modern probabilistic models based on comprehensive sets of new observations collected in all regions of the inner magnetosphere become available and are unified for all phases of the solar cycle.

[7] There are already a few new statistical and empirical RB models, such as CRRESPRO [*Meffert and Gussenhoven*, 1994], CRRESELE [*Gussenhoven et al.*, 1993, 1996], Low Altitude Trapped Radiation Model (LATRAM) [*Huston and Pfitzer*, 1998], Proton SAMPEX Belgian-Institute-for-Aeronomy 1997 (PSB97) [*Heynderickx et al.*, 1999], Trapped Proton Model 1 (TPM-1) [*Xapsos et al.*, 2002; *Huston*, 2002]. Most of these models have been compared to the early NASA models [*Lauerstein and Barth*, 2005]. They have not yet been validated and recommended by international organizations like the Committee on Space Research (COSPAR), the International Association of Geomagnetism and Aeronomy (IAGA), or International Organization for Standardisation (ISO). Consequently, they have not yet gained the same popularity as AE8 and AP8. Of course, to reach that level of repute would demand a lot of PR efforts emphasizing the real importance of this type of modeling activities, especially for space weather studies and design and operation of the next generations of Earth-orbiting satellites. Along these lines, novel indexes characterizing the Van Allen zones, like the "radiation belt content" (RBC), have been proposed recently by *Baker et al.* [2004].

[8] Most RB models are mapped using invariant coordinates which are derived from McIlwain's (B, L) drift shell parameters [*McIlwain*, 1961]. Indeed, these magnetic coordinates have proven to be most adequate to characterize and map the RB fluxes over the whole inner magnetosphere, thus sparing the need for longitude as a third spatial coordinate. Unfortunately, the (B, L) coordinates have a rather poor resolution at low altitudes between 100 and 2000 km. This limitation has been pointed out and deplored earlier by *Lemaire et al.* [1990a], *Heynderickx and Lemaire* [1996], *Daly et al.*, 1996, *Armstrong and Colborn* [2000], and *Huston* [2002]. A number of attempts have been made to improve upon this situation, i.e., to find a better coordinate system, other than (B, L), which would have a more adequate spatial resolution at low altitudes without, however, jeopardizing the good resolution at high altitudes. The aim of the present paper is to promote such an invariant coordinate that satisfies these requirements for the benefit of future space weather activities: the "invariant altitude," h_{inv}, which is a virtual altitude in McIlwain's reference dipole magnetic model.

[9] In the sections 2 and 3 we recall briefly the different coordinate systems generally used in RB mapping and modeling, and we illustrate the distributions of the standard NASA models using some of these most employed coordinates. In section 3 we introduce the definition of the invariant altitude and display a few orbits of SAMPEX, DEMETER, and CRRES using this novel invariant coordinate. The conclusions are drawn in section 4.

2. Invariant Coordinate Systems

[10] Since drift shells can be identified/labeled by pairs of adiabatic invariants of motion of charged particles drifting in the geomagnetic field, *McIlwain* [1961] introduced the magnetic invariant coordinates (B, L). These new magnetic coordinates replaced geographical and geodetic coordinates then used to map the fluxes of energetic particles forming the recently discovered Earth's radiation belts.

[11] The first drift shell coordinate, B, corresponds to the magnetic field intensity at the mirror point of the particles whose directional flux is measured at a point in space. The mirror point position is independent of the kinetic energy, provided that the gyroradius remains everywhere small compared to the characteristic length over which the magnetic field intensity changes and provided that it does not vary considerably over one gyroperiod. There are similar conditions associated with the interhemispheric bounce period and the period of revolution of trapped particles around the Earth. These conditions are Alfvén's conditions which were introduced by *Alfvén* [1940] and made popular in his book *Cosmic Electrodynamics* [*Alfvén*, 1950]. These conditions must be satisfied for the first-order orbit theory or guiding center approximation to be applicable and therefore for the magnetic moment of trapped particles to be an adiabatic invariant of motion. Under those conditions, the value of B at all mirror points is also an adiabatic invariant (at a first-order approximation).

[12] When Alfvén's conditions are satisfied, and when the momentum of trapped particles is conserved, there is a second adiabatic invariant of motion, I, the so-called longitudinal invariant. It is associated with the periodic oscillation (bounce motion) of trapped particles between conjugate mirror points. I is proportional to the line integral of the component of the particle momentum parallel to the magnetic field, integrated between mirror points. A drift shell of a trapped particle can be characterized by the pair of values B and I. Both quantities are calculated by using an appropriate mathematical model to approximate the geomagnetic field distribution at a given epoch (e.g., the International Geomagnetic Reference

Field (IGRF)/Definitive Geomagnetic Reference Field models).

[13] The (B, I) coordinates are transformed into (B, L) coordinates in a reference magnetic dipole that has been introduced by *McIlwain* [1961]. In this reference dipole field, L is the radial distance where the magnetic drift shell intersects the equatorial plane. The value of L is expressed in Earth radius (R_E = 6371.2 km). Drift shells in the McIlwain's dipole have the same value of I as the corresponding ones in the actual geomagnetic field. McIlwain's reference dipole is characterized by the standardized dipole moment M_d = 0.311653 Gauss R_E^3.

[14] For those who are not acquainted with McIlwain's transformation, we recall it in Appendix A. A simpler and faster algorithm was developed a decade later by *Hilton* [1971] to calculate L when B and I are known; this is also recalled in Appendix A, since it is not yet employed at all data centers.

[15] It should be emphasized again that no secular variations should ever be applied to the value M_d as was suggested by *Hilton* [1971] at the end of his brief report. Indeed, making the value of M_d dependent on the epoch would generate irretrievable confusion and inconsistency when building unified RB models from data collected over widely different periods of time; it would also generate intricate confusion among the users retrieving predicted fluxes from such heterogeneous RB models for any later epoch or mission dates [*Lemaire et al.*, 1990a, 1990b; *Heynderickx et al.*, 1996]. Another important recommendation by these authors is that the epoch of the IGRF geomagnetic field model used to develop any new RB model from new sets of observations should be clearly indicated in the documentation distributed with the codes of the new RB model.

[16] It is important to recall also that L is definitely not the equatorial distance where a geomagnetic field line crosses the geomagnetic equatorial plane; this was clearly emphasized by *McIlwain* [1961, 1966]. In McIlwain's 1966 article, other coordinates, like the invariant radial distance (R), the magnetic latitude (λ), the O'Brien's invariant latitude (Λ), and the Kaufman K parameter introduced by others, are also discussed.

[17] Also about one decade later, *Kluge and Lenhart* [1971] proposed to use B/B_0 instead of B. Indeed, they argued that this alternative variable offers a more compact way to define the matrix of elements characterizing RB models. B_0 is the magnetic field intensity of a drift shell in the equatorial plane of McIlwain's reference dipole: $B_0 = M_d/L^3$. The history of the various procedures used to calculate L and to map RB models is reviewed by *Heynderickx et al.* [1996].

[18] The (B, L) coordinates have been universally adopted, despite isolated efforts for promoting Euler coordinates (α and β), or other ''canonical coordinates'' to label drift shells [see *Schulz*, 1996]. The reason for the standing success of the (B, L) coordinates is that they are based on robust definitions, can be computed faster than some of these alternative coordinates, and because they have a straightforward geometrical meaning. Furthermore, since 1961, McIlwain's algorithm has been distributed freely all over the world, just as open source codes are nowadays, and it became available as a validated standard software in nearly all data centers around the world. It would seem mindless to abandon a coordinate system that has been so reliable in the past and that has been so intensively used in scientific publications for almost half a century. The original and correct computer subroutines calculating B, I, and L, as well as a variety of other useful coordinates (e.g., GSM and GEO) are freely available on the Internet at NSSDC and at the UNILIB Web site, http://www.oma.be/NEEDLE/unilib.php/. The Space Environment Information System (SPENVIS) employs these validated software codes through a user-friendly Web interface which is documented by *Heynderickx et al.* [1996, 2004].

3. Mapping of Radiation Belt Fluxes Using Invariant Coordinates

[19] Figure 1 illustrates the spatial distribution of omnidirectional fluxes for RB electrons (Figure 1a) and protons (Figure 1b) with energies exceeding 2 MeV. The B/B_0 and L coordinates are used here to map the integral fluxes predicted by the AE8-MAX and AP8-MAX models, respectively.

[20] The highest fluxes are located along the horizontal axis, where B/B_0 = 1, which corresponds to the equatorial plane in McIlwain's reference dipole. The maximum fluxes of the inner and outer Van Allen belts are located at about L = 1.5 and L = 4, respectively, for electrons with energies larger than 2 MeV. The center of the outer belt is at a larger L in the case of the AE8-MIN model, corresponding to average solar minimum conditions. The equatorial position of the peak flux depends also on the energy threshold: for lower energies, the maxima of the RB are located at larger L values.

[21] The upper border in Figures 1a and 1b corresponds to the low-altitude edge of the RB where the energetic particle fluxes drop to zero. This limit corresponds to the so-called atmospheric cutoff. This is where the atmosphere becomes sufficiently dense that the particles are removed from the trapping region by collisions. This level is located in the actual geomagnetic field at about 100 km, above the South Atlantic Anomaly (SAA); it is at higher altitude everywhere else. The SAA is where a high-inclination low Earth orbiting (LEO) spacecraft experiences the largest rate of single event upsets. It is currently located at about 35°S geographical latitude and 40°W longitude; it is shifting westward at a rate of $\sim$0.3° per year [*Lemaire et al.*,1995; *Dyer et al.*, 1996].

[22] The diamonds aligned along vertical lines in Figure 1 correspond to the data points stored in the matrix of the NASA models. In these models, the maximum flux at the magnetic equator, B/B_0 = 1, is listed for a discrete set of L parameters and for a discrete set of energy thresholds. They are followed by increasing values of B/B_0 where the

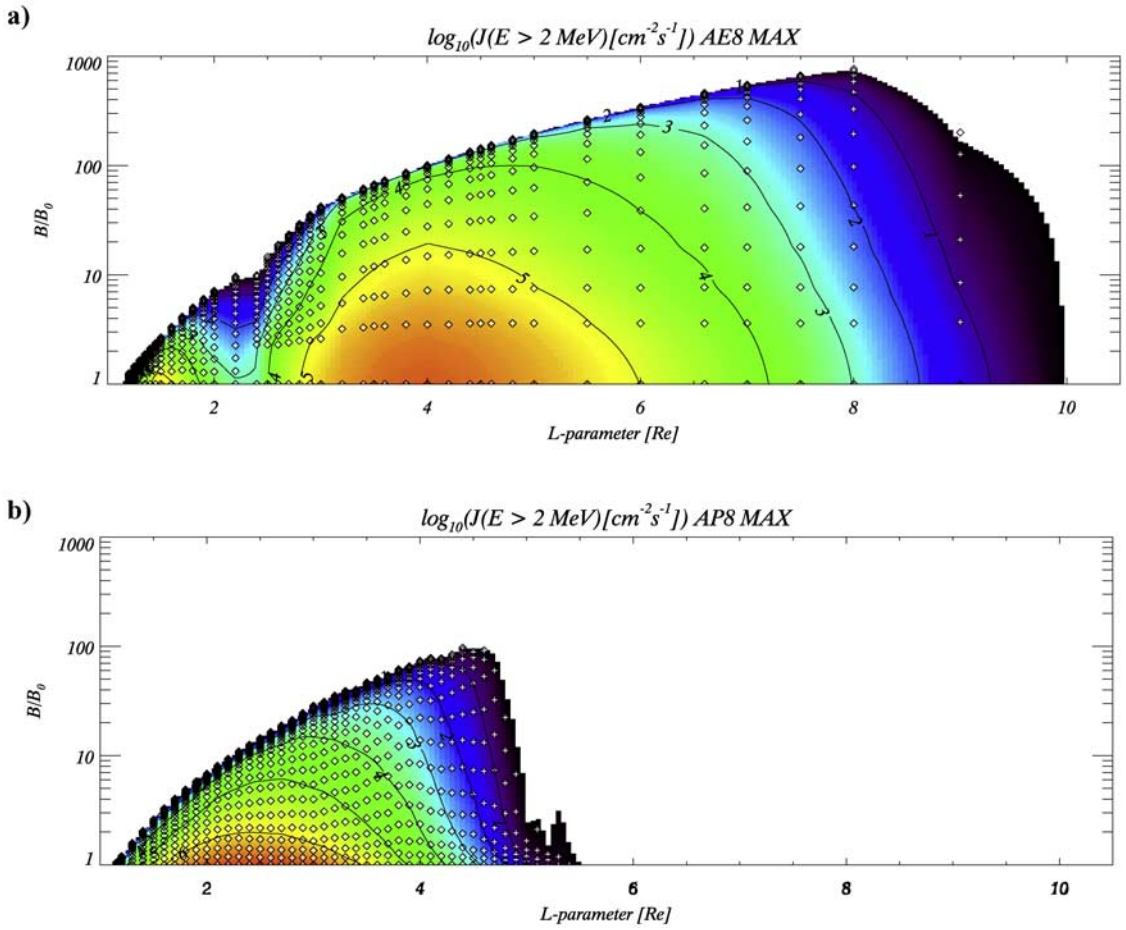

Figure 1. Omnidirectional fluxes $J(E > 2$ MeV) in cm^{-2} s^{-1}: (a) AE8-MAX for electrons and (b) AP8-MAX for protons with energies exceeding 2 MeV versus L (in R_E) and B/B_0. The contour lines correspond to the integer values of $\log_{10}(J)$. The diamonds are the locations where AE8-MAX and AP8-MAX flux values are given in the matrix representation of these empirical models; at other positions, the flux must be interpolated. The inner and outer electron belts are clearly outlined in Figure 1a; the equatorial peak of the proton flux distribution is shown in Figure 1b.

logarithm of the flux is decremented by a constant value. It was *Kluge and Lenhart* [1971] who introduced this special matrix representation for radiation belt models. This reduces the number of matrix elements necessary to characterize the flux distribution in RB models. It avoids also a standard rectangular mesh in the (B, L) space which jeopardizes the spatial resolution at low altitudes. Indeed, at low altitudes, the RB fluxes vary by large factors over one atmospheric density scale height (i.e., ~100 km), while the value of B does not change significantly over such a restricted altitude range. This new matrix format has been quickly adopted and integrated by *Teague et al.* [1972] to characterize all versions of the NASA models. Adapted interpolation subroutines had to be developed for accessing the new model versions, i.e., to evaluate the flux at any intermediate location in between the grid points of Figure 1. For details on these interpolations algorithms, see *Heynderickx et al.* [1996].

[23] From Figure 1, it can be seen that the distances between successive grid points become extremely small closer to the atmospheric cutoff where the trapped particle fluxes drop to zero. This is where the field-aligned distributions of trapped particle are directly controlled by the atmosphere, much more than by the geomagnetic field distribution. The density scale height in the upper Earth's atmosphere is of the order of 100 km and is a function of the thermospheric temperature.

[24] Since the values of B or B/B_0 do not vary significantly over a range of 100 km in altitude, the mesh points in (B/B_0, L) space cluster close to each other and fail to be well resolved in the low-altitude region. This is the reason why B or B/B_0 coordinates are not quite adequate for mapping of the RB at low altitudes, i.e., in the range where LEO missions like SAMPEX and DEMETER are currently collecting environmental data.

[25] As indicated above, this deficiency had been pointed out earlier, and novel coordinates were actively searched since 1986. But a fully satisfactory solution to this pending problem had yet to be identified. What is needed is an alternative spatial variable enabling mapping of the low-altitude environment with an expanded spatial resolution while keeping a satisfactory resolution at high altitudes as well.

[26] The equatorial pitch angle (α_0) has been introduced by *Heynderickx et al.* [1999] as a flux mapping coordinate. Unfortunately, this invariant coordinate suffers the same structural weakness as B and B/B_0; both coordinates are related to each other by

$$\sin^2(\alpha_0) = B_0/B.$$

[27] A modified invariant distance (R_{mod}) was introduced by *Huston* [2002], who uses a finer rectangular mesh with a width of 78 km at altitudes less than 637 km and a coarser mesh (780 km) at higher altitudes; the horizontal axis is the magnetic latitude, λ, with a constant spacing of $\Delta\lambda = 2^\circ$. This double-rectangular mesh of grid points is used to build the TPM-1 radiation belt model. This new RB model is based on the data sets from the medium energy proton and electron detector (MEPED) aboard TIROS/NOAA and on the CRRESPRO empirical model. From the point of view of the number of matrix elements required to store the RB fluxes, this grid is less economic than that used in the NASA models illustrated in Figure 1. The dispersion or standard deviation of measured particles fluxes in each bin vary discontinuously at the cross-over altitude in this inhomogeneous model. This inherent discontinuity of the standard deviations is a shortcoming of this model. However, the interpolation method in the (R_{mod}, λ) double-rectangular mesh might be viewed as an improvement over that used in the NASA models, except perhaps at the cross-over altitude.

[28] The minimum altitude of drift shells has been used by D. Heynderickx (private communication, 2004) to map SAMPEX/Proton-Electron Telescope (PET) flux measurements. The advantage of this alternative coordinate is not obvious, especially because of the much larger amount of computation necessary to calculate the minimum altitude of the drift shells generally located in the South Atlantic Anomaly.

[29] In section 4 we suggest an invariant coordinate that does not suffer these limitations, that meets the requirements outlined above, and that is more appropriate to bin data for LEO missions. It is surprisingly simple and requires only a very small extra number of computer resources beyond those currently used in RB modeling and data analysis.

4. Invariant Altitude: Alternative Coordinate for Mapping Low-Altitude Environmental Data

[30] In the seminal review by *McIlwain* [1966, p. 596], three specific ways had been recommended "to be particularly useful in exhibiting the information content of many different sets of data:

[31] (a) Contours of constant values of the dependent variable in (R, λ) space plotted in polar coordinates. Such plots can be used to exhibit the character of distributions in physical space.

[32] (b) Contours of constant values of the dependent variable in (B, L) space using a linear scale for L, and a logarithmic scale for B with one factor of ten in B corresponding to one Earth radius in L. The use of the log scale for B prevents the collapse of the equatorial region of high L values into a small area on the graph.

[33] (c) Particle fluxes versus B for constant values of L with logarithmic scales for both flux intensity and B, but with one factor of ten in B corresponding to four factors of ten in intensity."

[34] Unfortunately, these directives have rarely been followed by modelers, although it would have facilitated intercomparison between new models and the older ones. Of course, the same directives stand when B is replaced by B/B_0, i.e., the variable introduced by *Teague et al.* [1972]. Figure 1 is scaled according to McIlwain's directive b but with $\log_{10}(B/B_0)$ on the vertical axis instead of $\log_{10}(B)$.

[35] A number of functions of B and L have been introduced in the past to facilitate the handling, presentation, and understanding of data. Commonly used variables are R and λ, which are determined by

$$B = \frac{\mathrm{M_d}}{R^3}\left(4 - \frac{3R}{L}\right)^{1/2} \tag{1}$$

$$\cos^2\lambda = R/L, \tag{2}$$

where R is the radial distance in McIlwain's reference dipole, R is in units of Earth radius, and λ is the magnetic latitude in this reference B field. It is not possible to express R as a function of B and L in terms of known functions, but straightforward iterative numerical methods can be employed. However, *Roberts* [1964] found a more efficient method for calculating R when B and L are known. Roberts' method involves a minimum amount of numerical computation. Since it is not very well known, we recall it in Appendix A.

[36] In the present article we propose a new coordinate which is derived from R but which had not been suggested so far. This new coordinate is the "invariant altitude," h_{inv}. It is simply defined by

$$h_{\mathrm{inv}} = (R-1)R_e, \tag{3}$$

where R is obtained from B and L by using the Roberts method mentioned above or by the iterative method implemented in UNILIB.

[37] Thus it is rather straightforward to determine the value of $h_{\mathrm{inv}} = (R - 1)\,R_e$ when B and I or L have been

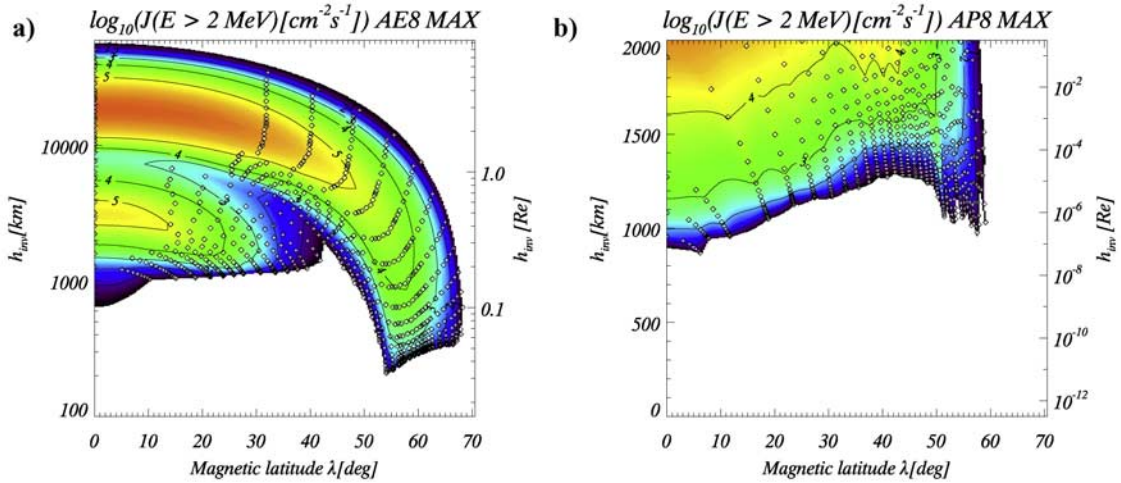

Figure 2. Omnidirectional fluxes $J(E > 2$ MeV) in cm^{-2} s^{-1}: (a) AE8-MAX for electrons and (b) AP8-MAX for protons with energies exceeding 2 MeV versus the magnetic latitude λ and the invariant altitude h_{inv}. The isocontour lines correspond to the integer values of $\log_{10}(J)$. The diamonds are the locations where AE8-MAX and AP8-MAX flux values are given in the matrix representation of these models; at other positions, the fluxes have been interpolated. Note in Figure 2b the wavy structure of some isocontours; this illustrates the limitation of the interpolation algorithms used with AP8 to determine the fluxes in between the mesh points at low altitudes.

derived for a point given its geodetic coordinates. In order to assign h_{inv} the meaning of an altitude, its value will be expressed in km and not in Earth radii as are R and L.

[38] A literal definition of the invariant altitude h_{inv} is the virtual altitude of the mirror points, in McIlwain's reference dipole, that have the same B and I or L coordinates as a drift shell in a model approximating the actual geomagnetic field distribution. In other words, h_{inv} is the altitude of the lower edges of the cylindrically symmetric drift shell in the reference dipole model. Since it is directly derived from B and I or L, which are invariant coordinates, h_{inv} is also an invariant coordinate.

[39] Figure 2a shows the distribution of electron fluxes ($E > 2$ MeV) from the AE8-MAX model, using a logarithmic scale for h_{inv} ranging from 100 to 60,000 km. A linear scale is used for λ ranging from 0° to 70°. Figure 2b displays the AP8-MAX flux model in the (h_{inv}, λ) coordinate system. A linear scale is used here for h_{inv} between 0 and 2000 km, in order to cover exclusively the low-altitude environment where LEO missions are in orbit.

[40] The diamonds correspond to the grid points displayed in the panels of Figure 1. They are again shown here to illustrate that at low-altitudes these grid points are now much more widely separated from each other in Figures 2a and 2b than they were in Figure 1. This illustrates the definite advantage of this new coordinate for displaying RB fluxes, as well as for binning RB data at low altitudes.

[41] Furthermore, note in Figure 2a that at high equatorial altitudes, around the center of the inner and outer radiation belts, the AE8 grid points remain well resolved when our new coordinate system is employed. For $\lambda < 10°$, the density of these grid points appears to be rather scarce and inadequate. It is clear that a rectangular mesh in λ and h_{inv} or $\log_{10}h_{inv}$ would cover more adequately the equatorial region around $\lambda < 10°$, i.e., where the flux values are largest but where, unfortunately, the density of the AE8 grid points happens to be rather scarce.

[42] To facilitate intercomparison between old and future new RB models, as well as the assimilation of new RB observations, we suggest using the format of Figure 2a, using a fixed log scale for h_{inv} (with h_{inv} ranging from 100 to 60,000 km) and a fixed linear scale for λ (ranging from 0° to 70°). Furthermore, when RB measurements are only restricted to the low-altitude region, we suggest use of a linear scale with h_{inv} ranging from 0 to 2000 km, as in Figure 2b. These formats could become new conventional ways for exhibiting the fluxes of trapped radiation belts observations, in addition to those proposed by *McIlwain* [1966] and recalled above.

[43] We recommend that most existing RB models currently available be remapped using these two formats: The first one with a linear scale for h_{inv} would be most appropriate for evaluating the fluxes, fluences, or doses for LEO missions, the standard deviations being then almost independent of altitude; the second format, with the logarithmic scale for h_{inv}, is more appropriate for the evaluation of these environmental parameters for high Earth orbit (HEO), geosynchronous transfer orbit (GTO), or geosynchronous orbit (GEO) missions. The error bars

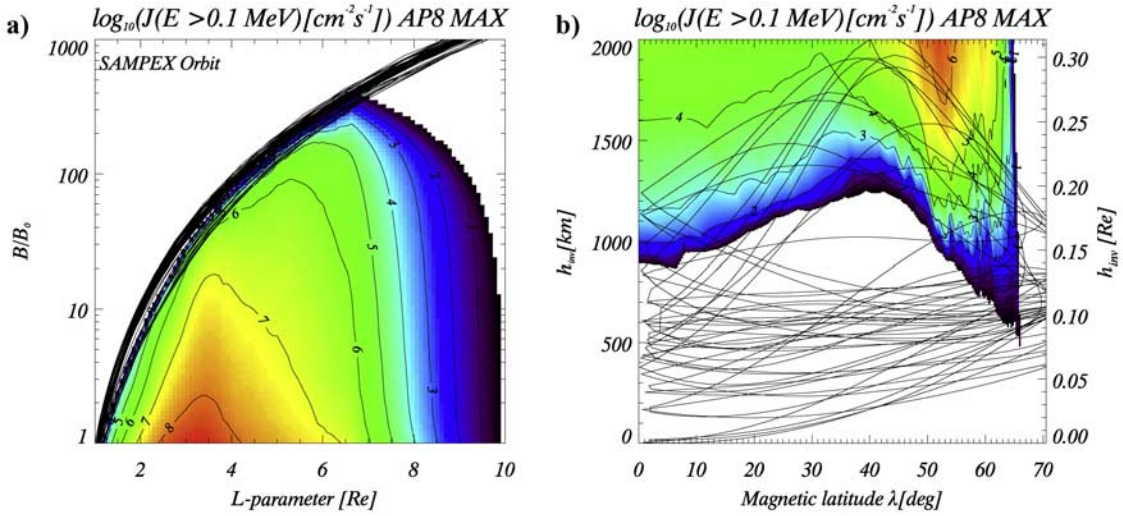

Figure 3. Comparison of 13 SAMPEX orbits (black lines) in two different coordinate systems: (a) same format as Figure 1b and (b) same format as Figure 2b but for proton energies above 0.1 MeV. It can be seen that in the (B/B_0, L) coordinates, the low-altitude orbits are much less well resolved than in the (h_{inv}, λ) coordinates used in Figure 3b.

of the binned/modeled particle fluxes is then an increasing function of altitude.

[44] To further illustrate the advantages of the invariant altitude as a new coordinate for mapping the RB environment, a series of 13 orbits of the SAMPEX satellite have been plotted in Figure 3, using both the old and new coordinate systems. The low-altitude orbits of the SAMPEX mission (apogee 675 km, perigee 550 km, inclination 82°) are displayed in Figure 3a, using the B/B_0 and L coordinates; the same set of orbits are also displayed in Figure 3b, using the h_{inv} and λ coordinates with the recommended linear scale for h_{inv}. These orbits are shown by the black curves and are superimposed on the isocontours of the AP8-MAX omnidirectional proton (> 0.1 MeV) fluxes.

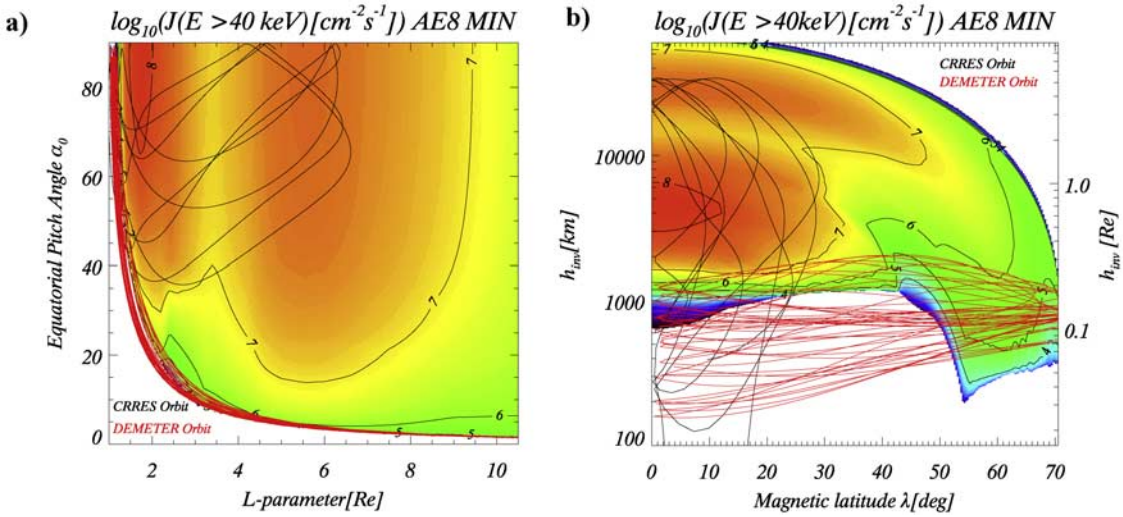

Figure 4. (a) Omnidirectional fluxes $J(E > 40$ keV) in cm^{-2} s^{-1} of electrons with energies exceeding 40 keV versus L (in R_E) and the equatorial pitch angle α_0. (b) Same as Figure 4a but using the magnetic latitude λ and the invariant altitude h_{inv} as a coordinate system. The isocontour lines correspond to integer values of $\log_{10}(J)$. Red lines are 13 orbits of the DEMETER satellite; black lines correspond to 20 orbits of the CRRES satellite on geosynchronous transfer orbit.

[45] It can be seen that the trajectories of this LEO spacecraft are spread over a much wider domain when the new invariant altitude coordinate is used as in Figure 3b than when the B/B_0 coordinate is used as for Figure 3a. As a matter of consequence, binning RB flux measurements using a rectangular mesh in Figure 3b will necessarily result in smaller standard deviations (i.e., smaller dispersion of flux values in all individual bins) than using a similar number of rectangular meshes in Figure 3a. Therefore a better spatial resolution will be achieved with the invariant altitude than with the B/B_0 coordinate; better statistical RB models will be obtained when this new coordinate is used to organize RB data sets.

[46] Similarly, in Figure 4, series of 13 low-altitude orbits of the DEMETER mission (circular orbit at an altitude of 710 km, inclination 98.23°), as well as a series of 20 orbits of the CRRES satellite are plotted. The CRRES mission on a highly elliptic GTO had an inclination of 18.15°, an apogee of 33,580 km, and a perigee of 350 km altitude. The α_0 and L coordinates are used in Figure 4a, while the h_{inv} and λ coordinates are used in Figure 4b, with our recommended logarithmic scale for h_{inv}. The isocontours of the AE8-MIN omnidirectional fluxes of electron (> 40 keV) fluxes are also shown for reference in Figures 4a and 4b.

[47] Once more, it can be seen that the trajectories of the LEO mission, DEMETER, are properly spread over a much wider area of the graph when the invariant altitude is used (Figure 4b) instead of the equatorial pitch angle (Figure 4a). When the h_{inv} and λ coordinates are used instead of α_0 and L, the trajectories of HEO and GTO missions are better resolved at low altitudes without jeopardizing their resolution at high altitude.

[48] These examples clearly indicate that mapping spatial distributions of fluxes of trapped particles is better displayed when using the invariant altitude defined by equation (3) instead of α_0 or B/B_0. A linear scale for h_{inv} ranging from 0 to 2000 km appears to be an appropriate format to map observations collected during LEO missions like SAMPEX and DEMETER. A logarithmic scale for h_{inv} ranging from 100 to 60,000 km appears to be a good alternative to map observations collected by HEO or GTO missions like CRRES. In both cases, a linear scale for the magnetic latitude, λ, ranging between 0° and 70° appears to be an appropriate choice for the abscissa. The invariant latitude which was introduced by *O'Brien et al.* [1962] might of course be an alternative, depending on the kind of application. Nevertheless, the magnetic latitude, λ, should be preferred in order to avoid empty regions in the graphs.

[49] To test these suggestions, we plan to bin the energetic electron flux measurements collected with the instrument for particle detection of the DEMETER mission [*Savaud et al.*, 2006] using this novel coordinate system. Furthermore, we envisage rebinning of available data sets from missions like SAMPEX/PET and OERSTED in order to study the secular variation of RB fluxes using this new coordinate. More elaborated empirical RB models based on probabilistic distributions functions should also be instrumented in the framework of this new invariant coordinate.

5. Conclusions

[50] After a brief overview of the different coordinate systems generally used to bin or map the fluxes of energetic electrons and protons trapped in the Van Allen belts, it has been shown that some of the invariant magnetic coordinates employed to label drift shells or to locate the positions of satellites are not well suited for all magnetospheric regions. For instance, the standard (B, L) and (α_0, L) coordinates are not well adapted to map observations from LEO missions. Indeed, the spatial resolution of the B coordinate is rather poor close to the atmospheric cutoff, where energetic particle fluxes drop sharply to zero over a small altitude range of only a few atmospheric scale heights (100–200 km).

[51] A more suitable set of coordinates has been searched for and investigated since 1986. Several alternative coordinates have been proposed over the last decade but with mitigated or limited success. The "invariant altitude," h_{inv}, proposed here as a new invariant magnetic coordinate has several advantages over other alternative coordinates used earlier for binning and mapping the radiation belt environment. It is quite straightforward to calculate from equation (3), and it definitely provides a better spatial resolution at low altitudes, where LEO missions are confined, without jeopardizing the resolution at high altitudes, where HEO, GTO, and GEO missions collect radiation belt observations. It might appear to be a rather small conceptual advance, but from preliminary mapping of observations of the LEO satellite DEMETER, it appears to be of greatest practical significance. It definitely improves the binning and mapping at low altitudes, where most of the other coordinates fail to provide an adequate spatial resolution.

[52] Figures 2, 3, and 4 illustrate some of the advantages of using the invariant altitude compared to other conventional invariant coordinates employed in the past. Two specific mapping formats have been proposed here to plot future as well as archived data to exhibit the spatial distribution of RB electron and proton fluxes. They should complement the three standard formats already recommended by *McIlwain* [1966].

[53] The calculation of the new coordinate, h_{inv}, requires only minimal additional computer resources beyond those used to compute the values of B and L. Indeed, h_{inv} is determined by the simple equation (3), where R is the radial distance in McIlwain's reference dipole. The value of R can easily be computed by using an algorithm published by *Roberts* [1964]. This algorithm is recalled in Appendix A. Validated FORTRAN code to compute R and

h_{inv} can be requested from the Center for Space Radiations from cabrera@spaceradiations.be.

Appendix A: Hilton's and Roberts' Algorithms to Calculate *L* and *R*, Respectively

A1. Calculation of the L Parameter

[54] *McIlwain* [1961]defined the magnetic shell parameter L for a point in the Earth's magnetic field by the equation

$$L^3B/M_d = F\left(I^3B/M_d\right) = F(X), \tag{A1}$$

where I is the invariant longitudinal integral, B is the mirror point field intensity, M_d is the Earth's dipole moment, and F is a function calculated for a dipole field. This function is represented as a set of polynomials of the form

$$\ln\left(L^3B/M_d - 1\right) = \sum_{n=0}^{6} c_n (\ln X)^n, \tag{A2}$$

where the constants c_n are given in a table by *McIlwain* [1961] for five different ranges in $X = I^3B/M_d$. This approximation of $F(X)$ gives L with an accuracy of 0.3% for all values of X and of 0.03% for $\ln X < 10$. In a subsequent review, *McIlwain* [1966] extended the polynomial expansion (A2) to 10 terms instead of 7, thus improving the accuracy with which the true value of L is approximated by this equation.

[55] A decade later, *Hilton* [1971] introduced a new approximation to calculate L when I and B are known. He approximated $F(X)$ by

$$L^3B/M_d = 1 + a_1X^{1/3} + a_2X^{2/3} + a_3X, \tag{A3}$$

where $a_1 = 1.35047$, $a_2 = 0.465376$, and $a_3 = 0.0475455$.

[56] Hilton's approximation significantly simplifies and improves the speed of the calculation of L. It results in a maximum error in the determination of L of less than 0.01% for all L and is asymptotically correct for $X \ll 1$ and $X \gg 1$. It is this approximation that is used in the UNILIB software package running at the Belgian Institute for Space Aeronomy, Brussels, and at the Centre for Space Radiations, Louvain-La-Neuve.

[57] For the sake of completeness, let us recall that since the Earth's magnetic moment is decreasing at a rate of 0.05% of the whole for a year, *Hilton* [1971] recommended that the value of M_d used in the determination of L be calculated from the dipole terms of the epoch dependent geomagnetic field model used in calculating B and the longitudinal integral I, while developing a new radiation belt model. Fortunately, it occurs that this recommendation has never been followed by experimenters and modelers. Indeed, not only does the dipole component of the IGRF have a secular variation, but the quadrupole and higher-order moments of the geomagnetic field also have significant secular variations. The latter produce a change in eccentric distance of the drift shells currently as large as 2.8 km/yr. Furthermore, the secular change of nondipole components led to a westward shift of the South Atlantic Anomaly at a rate of 0.34° per year [*Konradi et al.*, 1994; *Dyer et al.*, 1996].

[58] Thus, to avoid irretrievable confusion, it is recommended to use *McIlwain*'s [1961] original procedure with $M_d = 0.311653$ Gauss R_E^3 independently of epoch. In the final report of the Trapped Radiation Environment Model Development/European Space Research and Technology Center/Belgisch Instituut voor Ruimte-Aëronomie (TREND) project *Lemaire et al.* [1990b] emphasize that McIlwain's standard procedure must be maintained in future modeling activities to avoid possible confusion and unnecessary complications when retrieving prospective particle fluxes/spectra for any time in the future from a radiation belt model that would have been built with an epoch-dependent value for M_d. This is why in UNILIB this procedure is used and frozen in.

[59] It should be pointed out also that when the AE8-MIN and AP8-MIN radiation belt models are employed to evaluate energetic electron and proton fluxes/spectra for a period of minimum solar activity, the early *Jensen and Cain* [1962] geomagnetic field model must be used consistently. On the other hand, when such particles fluxes/spectra are needed for solar maximum, the GSFC12/66 geomagnetic field model [*Cain et al.*, 1967] must be used to calculate B and I when the AE8-MAX and AP8-MAX particle models are employed, since that is precisely the B field distribution attached to these NASA models [*Lemaire et al.*, 1990a, 1990b; *Heynderickx et al.*, 1996].

A2. Calculation of the Invariant Radial Distance, *R*

[60] Besides the widely used B and L invariant coordinates used for studying the particles trapped in the geomagnetic field, *McIlwain* [1961] also introduced the R and λ coordinates related to B and L by the equations

$$B = \left(M_d/L^3\right)\left(4 - 3\cos^2\lambda\right)^{1/2}/\cos^6\lambda \tag{A4}$$

$$R = L\cos^2\lambda, \tag{A5}$$

where R is the invariant radial distance (in Earth radii), and λ is the magnetic latitude in McIlwain's reference dipole.

[61] Equations (A4) and (A5) reveal that, though it is trivial to compute B and L given R and λ, the inverse transformation cannot be accomplished in terms of well-known functions. Besides standard but time-consuming iterative methods, *Roberts* [1964] found a simpler and faster algorithm that has not gained great popularity within the community of RB modelers. Nevertheless, it

should be recommended because of its accuracy and efficiency.

[62] Defining the parameters p and s by

$$p = \left(L^3 B/M_d\right)^{-1/3} \tag{A6}$$

$$\cos^2 \lambda = ps, \tag{A7}$$

equation (A4) reduces to

$$s^6 + 3ps - 4 = 0, \tag{A8}$$

which determines s as a function of the input parameter p whose value lies between 0 and 1. For this range $s(p)$ is a well-behaved function whose value monotonically decreases from $2^{1/3}$ to 1 for p changing from 0 to 1. Using Taylor series expansions of $s(p)$ at these limits, *Roberts* [1964] has been able to determine a least squares polynomial fit over the interval $0 < p < 1$. The best seventh-degree polynomial fit to $s(p)$, in the least squares sense, over this interval is given by

$$s(p) = \sum_{n=0}^{7} a_n p^n, \tag{A9}$$

where $a_0 = 1.25992106$, $a_1 = -0.19842592$, $a_2 = -0.04686632$, $a_3 = -0.01314096$, $a_4 = -0.00308824$, $a_5 = 0.00082777$, $a_6 = -0.00105877$ and $a_7 = 0.00183142$.

[63] The error made by evaluating $s(p)$ with equation (A9) is everywhere less than $0.5\ 10^{-7}$ in the entire interval $0 < p < 1$. By equation (A7), this corresponds to a fractional error of about 0.2×10^{-7} in evaluating $\cos \lambda$ and 0.4×10^{-7} in evaluating R from equation (A5). A FORTRAN 77 computer subroutine for converting from (B, L) to (R, λ) based on Robert's method can be requested from Juan Cabrera (cabrera@spaceradiations.be).

[64] **Acknowledgments.** The authors are members of the Center for Space Radiations, Louvain-La-Neuve, Belgium. This study has been supported by the grant PRODEX/contract 90179 from BELSPO, the space department of the Belgian Federal Science Policy Office, as well as through the logistic support from the Department of Physics at the University Catholique de Louvain. The authors wish to acknowledge discussions with Mathias Cyamukungu of CSR and Daniel Heynderickx of BISA. Inputs from Paul O'Brien, Aerospace Corporation, and Carl McIlwain, UCSD, have been particularly appreciated. We thank also Sylvie Benck, CSR, for careful editing of the final manuscript.

References

Alfvén, H. (1940), On the motion of a charged particle in a magnetic field, *Ark. Mat. Astron. Fysik*, *27A*(22), 1–3.

Alfvén, H. (1950), *Cosmic Electrodynamics*, Oxford Univ. Press, New York.

Armstrong, T. W., and B. L. Colborn (2000), TRAP/SEE code users manual for predicting trapped radiation environments, *NASA Contract. Rep. NASA/CR-2000-209879*.

Baker, D. N., S. G. Kanekal, and J. B. Blake (2004), Characterizing the Earth's outer Van Allen zone using a radiation belt content index, *Space Weather*, *2*, S02003, doi:10.1029/2003SW000026.

Beliaev, A. A., and J. F. Lemaire (1996), Comparison between NASA and INP/MSU radiation belt models, in *Radiation Belts: Models and Standards*, *Geophys. Monogr. Ser.*, vol. *97*, edited by J. F. Lemaire, D. Heynderickx, and D. N. Baker, pp. 141–145, AGU, Washington, D. C.

Bourdarie, S., R. H. W. Friedel, J. Fennell, S. Kanekal, and T. E. Cayton (2005), Radiation belt representation of the energetic electron environment: Model and data synthesis using the Salammbô radiation belt transport code and Los Alamos geosynchronous and GPS energetic particle data, *Space Weather*, *3*, S04S01, doi:10.1029/2004SW000065.

Cain, J. C., S. J. Hendricks, R. A. Langel, and W. V. Hudson (1967), A proposed model for the International Geomagnetic Reference Field—1965, *J. Geomagn. Geoelectr.*, *19*, 335–355.

Daly, E. J., J. Lemaire, D. Heynderickx, and D. J. Rodgers (1996), Problems with models of the radiation belts, *IEEE Trans. Nucl. Sci.*, *43*, 403–415.

Dyer, C., A. Sims, and C. Underwood (1996), Radiation belt observations from CREAM and CREDO, in *Radiation Belts: Models and Standards*, *Geophys. Monogr. Ser.*, vol. *97*, edited by J. F. Lemaire, D. Heynderickx, and D. N. Baker, pp. 229–236, AGU, Washington, D. C.

Fung, S. F. (1996), Recent development in NASA trapped radiation models, in *Radiation Belts: Models and Standards*, *Geophys. Monogr. Ser.*, vol. *97*, edited by J. F. Lemaire, D. Heynderickx, and D. N. Baker, pp. 79–91, AGU, Washington, D. C.

Gussenhoven, M. S., E. G. Mullen, M. D. Violet, C. Hein, J. Bass, and D. Madden (1993), CRRES high energy proton flux maps, *IEEE Trans. Nucl. Sci.*, *40*, 1450–1457.

Gussenhoven, M. S., E. G. Mullen, and D. H. Brautigam (1996), Phillips Laboratory, Space Physics Division radiation models, in *Radiation Belts: Models and Standards*, *Geophys. Monogr. Ser.*, vol. *97*, edited by J. F. Lemaire, D. Heynderickx, and D. N. Baker, pp. 93–101, AGU, Washington, D. C.

Heynderickx, D., and J. Lemaire (1996), Coordinate systems for mapping low-altitude trapped particle fluxes, *AIP Conf. Proc.*, *383*, 187–192.

Heynderickx, D., J. Lemaire, and E. J. Daly (1996), Historical review of the different procedures used to compute the *L*-parameter, *Radiat. Meas.*, *26*(3), 325–331.

Heynderickx, D., M. Kruglanski, V. Pierrard, J. Lemaire, M. D. Looper, and J. B. Blake (1999), A new low-altitude trapped proton model for solar minimum conditions based on SAMPEX/PET data, *IEEE Trans. Nucl. Sci.*, *46*, 1475–1480.

Heynderickx, D., B. Quaghebeur, J. Wera, E. J. Daly, and H. D. R. Evans (2004), New radiation environment and effects models in the European Space Agency's Space Environment Information System (SPENVIS), *Space Weather*, *2*, S10S03, doi:10.1029/2004SW000073.

Hilton, H. H. (1971), *L* parameter: A new approximation, *J. Geophys. Res.*, *76*, 6952–6954.

Huston, S. L. (2002), Space environment and effects: Trapped proton model, *NASA Contract. Rep. NASA/CR-2002-211784*.

Huston, S. L., and K. A. Pfitzer (1998), Space environment effects: Low-altitude trapped proton model, *NASA Contract. Rep. NASA/CR-1998-208593*.

Jensen, D. C., and J. C. Cain (1962), An interim geomagnetic field, *J. Geophys. Res.*, *67*, 3568–3569.

Kluge, G., and K. G. Lenhart (1971), A unified computing procedure for trapped radiation models, *ESOC Internal Note 78*, Eur. Space Oper. Cent., Darmstadt, Germany.

Konradi, A., G. D. Badhwar, and L. A. Braby (1994), Recent space shuttle observations of the South Atlantic Anomaly and the radiation belt models, *Adv. Space Res.*, *14*(10), 911–921.

Lauerstein, J.-M., and J. L. Barth (2005), Radiation belt modelling for spacecraft design: Model comparisons for common orbits, paper presented at 2005 Radiation Effects Data Workshop, Inst. of Electr. and Electron. Eng., Seattle, Washington, 11–15 July.

Lemaire, J., E. J. Daly, J. I. Vette, C. E. McIlwain, and S. McKenna-Lawlor (1990a), Secular variations in the geomagnetic field and calculations of future low-altitude radiation environments, in *Proceedings of ESA Workshop on Space Environment Analysis*, *ESA-WPP-23*, pp. 1–16, Eur. Space Res. and Technol. Cent., Noordwijk, Netherlands.

Lemaire, J., et al. (1990b), Development of improved models of the Earth's radiation environment, *Tech. Notes 1–6, Final Rep. Contract ESTEC 9011/88/NL/MAC*, Belg. Inst. for Space Aeron., Brussels.

Lemaire, J., A. D. Johnstone, D. Heynderickx, D. J. Rodgers, S. Szita, and V. Pierrard (1995), Trapped Radiation Environment model development, TREND-2 final report, *Aeron. Acta A*, *393*, 1–249.

McIlwain, C. E. (1961), Coordinates for mapping the distribution of geomagnetically trapped particles, *J. Geophys. Res.*, *66*, 3681–3691.

McIlwain, C. E. (1966), Magnetic coordinates, *Space Sci. Rev.*, *5*, 585–598.

Meffert, J. D., and M. S. Gussenhoven (1994), CRRESPRO documentation, *PL-TR-94-2218*, *Environ. Res. Pap. 1158*, Air Force Res. Lab., Wright-Patterson Air Force Base, Ohio.

O'Brien, T. P. (2005), A framework for next-generation radiation belt models, *Space Weather*, *3*, S07B02, doi:10.1029/2005SW000151.

O'Brien, B. J., C. D. Laughin, J. A. Van Allen, and L. A. Frank (1962), Measurements of the intensity and spectrum of electrons at 1000 kilometer altitude and high latitudes, *J. Geophys. Res.*, *67*, 1209–1225.

Roberts, C. S. (1964), Coordinates for the study of particles trapped in the Earth's magnetic field: A method of converting from B, L to R, λ coordinates, *J. Geophys. Res.*, *69*, 5089–5090.

Savaud, J. A., T. Moreau, R. Maggiolo, J.-P. Treilhou, C. Jacquey, A. Cros, J. Coutelier, J. Rouzaud, E. Penou, and M. Gangloff (2006), High-energy electron detection onboard DEMETER: The IDP spectrometer, description and first results on the inner belt, *Planet. Space Sci.*, *54*, 502–511, doi:10.1016/j.pss 2005.10.019.

Schulz, M. (1996), Canonical coordinates for radiation belt modeling, in *Radiation Belts: Models and Standards*, *Geophys. Monogr. Ser.*, vol. *97*, edited by J. F. Lemaire, D. Heynderickx, and D. N. Baker, pp. 153–160, AGU, Washington, D. C.

Teague, M. J., J. Stein, and J. I. Vette (1972), The use of the inner zone electron model AE-5 and associated computer programs, *ANSSDC/WDC-A-R & S 72-11*, Natl. Space Sci. Data Cent., NASA Goddard Space Flight Cent., Greenbelt, Md.

Vette, J. I. (1991), The AE-8 trapped electron model environment, *NSSDC/WDC-A-R&S 91-24*, Natl. Space Sci. Data Cent., NASA Goddard Space Flight Cent., Greenbelt, Md., Nov.

Xapsos, M. A., S. L. Huston, J. L. Barth, and E. G. Stassinopoulos (2002), Probabilistic model for low-altitude trapped-proton fluxes, *IEEE Trans. Nucl. Sci.*, *49*, 2776–2781.

J. Cabrera and J. Lemaire, Centre for Space Radiations, Chemin du Cyclotron, 2, B-1348, Louvain-la-Neuve, Belgium. (cabrera@spaceradiations.be; jfl@astr.ucl.ac.be)